*The FASEB Journal*

FASEB
Federation of American Societies for Experimental Biology

RESEARCH ARTICLE OPEN ACCESS

# Focal Adhesion Kinase Orchestrates GLUT4 Translocation and Glucose Uptake via Cytoskeletal Turnover in Primary Adipocytes

Franziska Kopietz[1] | Mathis Neuhaus[1] | Andrea Borreguero-Muñoz[1] | Dmytro Kryvokhyzha[2] | Karin G. Stenkula[1]

[1]Department of Experimental Medical Science, Medical Faculty, Lund University, Lund, Sweden | [2]Department of Clinical Sciences, Lund University Diabetes Centre, Malmö, Sweden

**Correspondence:** Karin G. Stenkula (karin.stenkula@med.lu.se)

**Received:** 14 January 2025 | **Revised:** 18 April 2025 | **Accepted:** 12 May 2025

**Funding:** This work was supported by the Swedish Research Council (2023-01779) and Strategic Research Area EXODIAB (2009-1039), the Swedish Foundation for Strategic Research (IRC15-0067), Novo Nordisk (NNF20OC0063659), Swedish Diabetes Foundation, The Royal Physiographic Society of Lund, and Albert Påhlsson Foundation.

**Keywords:** actin | adipocytes | cytoskeleton | FAK | focal adhesion kinase | glucose uptake | GLUT4 | insulin

## ABSTRACT

Intact insulin signaling and glucose transport in adipocytes are crucial to maintaining whole-body energy metabolism. Focal adhesion kinase stands as a central intracellular protein facilitating signaling between the extracellular matrix and the cytoplasm, thereby regulating cellular metabolism. Here, we have investigated the role of focal adhesion kinase in adipocyte glucose transport using an array of methods, including affinity purification combined with quantitative mass spectrometry, glucose tracer assays, western blotting, and confocal imaging. Pharmacological inhibition (PF-573228) of focal adhesion kinase suppressed the interaction of focal adhesion kinase with numerous actin-associated proteins, reduced Rac1 activity, as well as phosphorylation of the Rac1 downstream target PAK1/2, and further led to impaired GLUT4 translocation and glucose uptake. In summary, we demonstrate that focal adhesion kinase plays a key role in controlling actin remodeling, subsequent GLUT4 translocation, and ultimately glucose transport in adipocytes.

## 1 | Introduction

Intact insulin signaling and glucose transport in adipocytes are central for maintaining whole-body energy metabolism [1]. Despite decades of research, the etiology of insulin resistance is not yet resolved. Impaired translocation of the main insulin-responsive glucose transporter 4 (GLUT4) has been proposed as the ultimate defect in insulin resistance [2]. GLUT4 translocation and fusion of GLUT4 storage vesicles with the plasma membrane are processes tightly regulated by an intricate balance of intracellular actin turnover [3–5]. Actin turnover is controlled by a signaling cascade initiated at transmembrane receptors (integrins), which participate in the communication between the extracellular matrix (ECM) and the cytoplasm [6, 7]. Impaired cytoskeletal reorganization, as well as ECM-related diseases (e.g., fibrosis),

**Abbreviations:** AS160, Akt substrate of 160 kDa; BSA, bovine serum albumin; DMSO, dimethyl sulfoxide; ECM, extracellular matrix; ERK1/2, Extracellular signal-regulated kinases 1/2; FAK, focal adhesion kinase; GLUT4, glucose transporter 4; IRS-1, insulin receptor substrate 1; PAK, p21-activated kinase; PKB, protein kinase B; Rac1, Rac Family Small GTPase 1.

Franziska Kopietz and Mathis Neuhaus contributed equally to this work.

have been linked to deteriorated insulin signaling and impaired GLUT4 translocation in the expanding adipose tissue [8–10].

Focal adhesion kinase (FAK) stands as a central intracellular protein facilitating signaling between the ECM and the cytoplasm. FAK is a non-receptor tyrosine kinase widely known for its role in cell migration [11]. Multiple studies have highlighted the role of FAK in cytoskeletal remodeling [12, 13], insulin signaling [14–17], and GLUT4 translocation [12, 18] in skeletal muscles, while research investigating these relations in adipocytes is limited. Instead, studies have addressed the influence of FAK on adipose tissue expansion and inflammation. For example, Luk et al. demonstrated that adipocyte-specific FAK knockout in mice is associated with reduced adipocyte survival, impaired adipose tissue expansion, and the onset of systemic insulin resistance [17]. In agreement, Ding et al. proposed that adipocyte FAK knockout in mice promoted adipose tissue inflammation, which in turn triggered beta-cell apoptosis and diabetes progression [19]. Shin et al. demonstrated that FAK signaling is essential to stabilize peroxisome proliferator-activated receptor gamma, which in turn ensures adipogenesis and "healthy" adipose expansion [20]. Both genetic and diet-induced obesity in mice, as well as observations in human subjects, have shown that FAK signaling is altered in enlarged adipose tissue [17, 20, 21]. Still, the role of FAK in regulating insulin signaling, GLUT4 dynamics, and glucose uptake at the cellular level in adipocytes remains largely unknown.

Herein, we explored the impact of acute pharmacological FAK inhibition on key mechanisms mediating insulin-stimulated glucose uptake in both rodent and human primary adipocytes.

## 2 | Materials and Methods

### 2.1 | Antibodies

Antibodies used for western blotting (WB), immunoprecipitation (IP), and confocal microscopy (CM) are provided in Table 1.

### 2.2 | Animals

Male C57BL/6J mice (Taconic, Ry, Denmark) were housed at the local animal facility with a 12 h light/dark cycle and non-restricted access to water and food. Mice were fed a chow diet SAFEA30 (SAFE Complete Care Competence). Ages ranged from 8 to 14 weeks. All animal procedures were reviewed and approved by the Malmö /Lund Committee for Animal Experiment Ethics, approval number 5.8.18-00497/2020.

### 2.3 | Human Adipose Tissue

Abdominal subcutaneous adipose tissue was collected from women who underwent reconstructive breast surgery at Scania University Hospital in Sweden. The participants were given written and oral information about the study before providing their informed, written consent. Human studies were approved by the Regional Ethical Review Boards at Lund University (approval number 2017/920).

### 2.4 | Adipocyte Isolation

Primary adipocytes were isolated from inguinal and epididymal mouse or human subcutaneous adipose tissue depots using

**TABLE 1** | Antibodies used for western blotting (WB), immunoprecipitation (IP), and confocal microscopy (CM).

| Target | Supplier | Article No. | RRID | Dilution | Notes |
|---|---|---|---|---|---|
| AS160 | Cell Signaling | 2670 | RRID:AB_2199375 | 1:1000 | WB |
| AS160 T642 | Cell Signaling | 4288 | RRID:AB_10545274 | 1:500 | WB |
| FAK | Cell Signaling | 13 009 | RRID:AB_2798086 | 1:1000 | WB |
| FAK | Cell Signaling | 3285 | RRID:AB_2269034 | 1:50 | IP |
| FAK Y397 | Cell Signaling | 8556 | RRID:AB_10891442 | 1:500 | WB |
| HSP90 | BD Biosciences | 610 418 | RRID:AB_397798 | 1:2000 | WB |
| PKB S473 | Cell Signaling | 4060 | RRID:AB_2315049 | 1:1000 | WB |
| PKB | Cell Signaling | 4691 | RRID:AB_915783 | 1:1000 | WB |
| IRS-1 | Cell Signaling | 3407 | RRID:AB_2127860 | 1:250 | WB |
| IRS-1 Y612 | Thermo Fisher | 44-816G | RRID:AB_1501247 | 1:500 | WB |
| ERK1/2 T202/Y204 | Cell Signaling | 4370 | RRID:AB_2315112 | 1:1000 | WB |
| Phospho-PAK1 (T423)/PAK2 (T402) | Cell Signaling | 2601 | RRID:AB_330220 | 1:1000 | WB |
| Arp2 (phospho T237 + T238) | Abcam | ab119766 | RRID:AB_10900743 | 1:250 | WB |
| Phospho-Cofilin (S3) | Cell Signaling | 3313 | RRID:AB_2080597 | 1:500 | WB |
| LM048 | Integral Molecular | CSB0148 | RRID:AB_3106913 | 1:300 | CM |
| α-Tubulin | Sigma-Aldrich | CP06 | RRID:AB_2617116 | 1:300 | CM |

collagenase digestion according to a previously established protocol [22]. Isolated primary adipocytes were suspended in Krebs Ringer Bicarbonate HEPES (KRBH) buffer, pH 7.4, containing 200 nM adenosine and 3% (w/v) bovine serum albumin (BSA) and washed three times in KRBH before being subjected to subsequent analyses.

### 2.5 | Inhibitor/Activator Treatment

Isolated adipocytes were pre-incubated for 1 h with the indicated concentrations of the FAK inhibitor PF-573228 (CS-3375, ChemScene, USA) dissolved in 100% dimethyl sulfoxide (DMSO) or the respective amount of DMSO. Thereafter, cells were either insulin-stimulated (10 nM insulin) or remained unstimulated before further analyses.

For Arp2/3 complex inhibition, isolated adipocytes were pre-incubated for 5 min with the indicated concentrations of CK666 (HY-16926, MedChemExpress, USA) or the respective amount of DMSO. Thereafter, cells were either insulin-stimulated (10 nM insulin) or remained unstimulated before further analyses.

For activation of Rac1, we used the Rho/Rac/Cdc42 activator CN04 (Cat. # CN04, Cytoskeleton Inc., Denver, USA) diluted in water. Isolated adipocytes were pre-incubated for 1 h with 1 μg/mL CN04. Thereafter, cells were either insulin-stimulated (10 nM insulin) or remained unstimulated before further analyses.

### 2.6 | Western Blot Analysis

After treatment, cells were washed three times in BSA-free KRBH and were then lysed 1:1 in a lysis buffer containing 50 mM Tris/HCl pH 7.5, 1 mM EGTA, 1 mM EDTA, 0.27 M sucrose, 1 mM Na-orthovanadate, 50 mM NaF, 5 mM Na-pyrophosphate, 1% (v/v) NP-40, 1 mM DTT, and a complete protease inhibitor cocktail (Roche, Basel, Switzerland). Lysates were centrifuged for 10 min at 13 000×*g* and bradford measurement was used to determine the total protein content. Equal amounts of protein were loaded on Criterion TGX Precast Gels (Bio-Rad Laboratories Inc.). Secondary antibodies used were anti-rabbit (No. 314060, Thermo Fisher Scientific, Waltham) and anti-mouse (No. NXA9311ML, Cytiva, Marlborough) horseradish peroxidase-conjugated secondary antibodies diluted at 1:2500 and 1:2000, respectively.

### 2.7 | Glucose Uptake

Glucose uptake was determined as previously described [23]. Briefly, isolated adipocytes were incubated with or without 10 nM insulin in KRBH buffer for 30 min, and thereafter D-14C(U)-glucose (2.5 μL/mL, NEC042, Perkin Elmer, Waltham) was added for an additional 30 min. The uptake was terminated by spinning 300 μL of each cell suspension in microtubes containing 75 μL dinonylphtalate oil. Cell fractions of about 9–15 μL packed cells were dissolved in scintillation fluid (Ultima Gold, Perkin Elmer) for scintillation counting.

### 2.8 | Immunoprecipitation

For immunoprecipitation, cell lysates (300 μg protein/sample) were incubated with FAK antibody (Cell Signaling 3285, 1:50) conjugated to protein A/G sepharose beads (pre-washed with lysis buffer containing 50 mM Tris–HCl pH 7.5, 1 mM EDTA, 1 mM EGTA, 1% [v/v] NP40, 1 mM Na-orthovanadate, 50 mM NaF, 5 mM Na-pyrophosphate, 0.27 M sucrose, 0.5 M NaCl, 1 mM DTT, and diluted 1:2). Rabbit IgG was used as a negative control. Protein lysates and beads were incubated for 2 h on a shaking platform at 4°C and thereafter prepared for quantitative mass spectrometry and western blot analysis.

### 2.9 | Sample Preparation for Mass Spectrometry (MS)

For MS analysis, the immunoprecipitated samples were washed with 50 mM Tris–HCl, pH 7.5, prior to on-bead digestion following Cho et al. [24]. Briefly, to retrieve the captured proteins, 1 mM dithiothreitol (DTT) in 2 M urea and 100 mM ammonium bicarbonate was added to the beads, followed by the addition of 0.5 μg sequencing grade trypsin (Promega, V5111). The samples were incubated at 25°C, 1000 rpm, for 2 h. The supernatant was retrieved, and the beads were washed with buffer containing 2 M urea and 100 mM ammonium bicarbonate, with the subsequent combining of the washes with the on-bead digest supernatant. The samples were reduced using 4 mM DTT (25°C, 1000 rpm, 30 min) followed by alkylation with 10 mM iodoacetamide (IAA) (25°C, 1000 rpm, 45 min). The samples were subsequently digested using an additional 0.5 μg sequencing grade trypsin overnight (25°C, 1000 rpm, 18 h). The digested samples were acidified with 10% formic acid to a final pH of 3.0, and the peptides were purified and desalted using C18 reverse-phase columns (The Nest Group Inc.) following the manufacturer's recommendations. Dried peptides were reconstituted in 2% acetonitrile and 0.1% formic acid prior to MS analysis.

### 2.10 | Liquid Chromatography–Tandem Mass Spectrometry (LC–MS/MS)

The peptides were analyzed on an Orbitrap Eclipse mass spectrometer connected to an ultra-high-performance liquid chromatography Dionex Ultra300 system (both Thermo Scientific). The peptides were loaded and concentrated on an Acclaim PepMap 100 C18 precolumn (75 μm × 2 cm) and then separated on an Acclaim PepMap RSLC column (75 μm × 25 cm, nanoViper, C18, 2 μm, 100 Å) (both columns Thermo Scientific) at a column temperature of 45°C and a maximum pressure of 900 bar. A linear gradient of 3%–25% of 80% acetonitrile in aqueous 0.1% formic acid was run for 50 min followed by a linear gradient of 25%–40% of 80% acetonitrile in aqueous 0.1% formic acid for 10 min. One full MS scan (resolution 120 000; mass range of 350–1400 m/z) was followed by MS/MS scans (resolution 15 000) with a 3 s cycle time. Precursors with a charge state of 2–6 were included. The precursor ions were isolated with a 1.6 m/z isolation window and fragmented using higher-energy collisional-induced dissociation (HCD) at

a normalized collision energy (NCE) of 30. The dynamic exclusion was set to 30 s.

### 2.11 | Mass Spectrometry Data Analysis

Raw mass spectrometry data were analyzed with Proteome Discoverer 2.5. The acquired spectra were analyzed against an in-house compiled dataset containing the *Mus musculus* reviewed reference proteome (UniProt proteome ID UP000005640) containing a total of 17079 protein entries. Fully tryptic digestion was used, allowing for two missed cleavages. Carbamidomethylation (C) was set to static, and protein N-terminal acetylation and oxidation (M) to variable modifications. The mass tolerance for precursor ions was set to 10 ppm, and for fragment ions to 0.02 Da. The protein false discovery rate (FDR) was set to 1%. Proteins identified by two or more unique peptides were considered relevant, whereas others were discarded.

The immunoprecipitation-mass spectrometry (IP-MS) data consisting of 711 proteins were filtered to retain those identified in all replicates of at least one condition, resulting in 666 proteins. The experiment included three biological replicates in three conditions: (1) untreated adipocytes (DMSO control), (2) treated with 10 nM insulin (DMSO INS), and (3) treated with 10 nM insulin and 10 μM FAK inhibitor (PF INS). As a negative control, three samples with IgG antibodies instead of FAK antibodies (IgG DMSO) were used, though one IgG DMSO sample was excluded from the analysis as an outlier in quality control metrics. Differential enrichment analysis was performed using the DEP package (version 1.26.0) [25], with significant differentially enriched proteins defined as those having an FDR $<0.05$ and a log2 fold change $>0.5$. Significant proteins were further analyzed for protein–protein interactions and gene ontology (GO) enrichment using STRING [26]. The GO enrichment analysis was conducted using a custom background of the 666 proteins to identify significant biological processes, molecular functions, and cellular components.

### 2.12 | Confocal Microscopy

Cells were fixed with 4% paraformaldehyde for 7 min at room temperature and subsequently washed twice with PBS. Samples were blocked with blocking buffer (1% BSA, 1% goat serum in KRBH) for 30 min and incubated with primary antibody GLUT4 LM048 [27] for 1 h, washed three times with PBS, and then incubated with AlexaFluor-labeled secondary antibodies. F-actin imaging was performed using Alexa Fluor Plus 647 Phalloidin (A30107, Invitrogen). F-actin tracers increase upon high-fat diet (HFD) treatment and are easily detectable. Therefore, we studied the effect of FAKi on F-actin formation in primary adipocytes isolated after 10 weeks of HFD feeding (D12492, 60% fat, Research Diets, New Brunswick, USA). Imaging was performed using a Nikon A1 Plus confocal microscope with a ×20 Plan Apo objective with NA of 0.75 (Nikon Instruments Inc., Danderyd, Sweden). Images were acquired with NIS-elements, version 4.50.02 (Laboratory Imaging, Danderyd, Sweden). Note, adipocytes isolated from inguinal adipose tissue were used for all analyses except LM048 confocal imaging (Figure 3H), where we used epididymal adipocytes. Corresponding glucose tracer assays were performed in epididymal adipocytes to confirm a consistent effect of FAKi on glucose uptake (Figure S1A). Imaging was performed blinded.

### 2.13 | RAC1 Activity Assay

Rac1 activity was measured in isolated inguinal adipocytes after pre-treatment with 10 μM FAKi or DMSO for 1 h and subsequent non- or 10 nM insulin stimulation for 5 min in KRBH without BSA. Cells were washed once in KRBH without BSA and immediately lysed 1:4 in GL36 lysis buffer (Cytoskeleton Inc., Denver, USA), centrifuged for 1 min at 10000×*g* and snap-frozen in liquid nitrogen. Protein concentrations were determined using precision red, and all lysates were diluted to a protein concentration of 0.6 mg/mL in GL36 lysis buffer. Aliquots of 50 μL lysate per well were used in technical duplicates in a G-LISA assay to determine Rac1 GTP loading according to the manufacturer's protocol (Rac1 G-LISA Activation Assay Kit (Colorimetric Based) 96 Assays #BK128, Cytoskeleton Inc). Absorbance was measured at 490 nm using a FLUOstar Omega microplate reader (BMG Labtech, Ortenberg, Germany).

### 2.14 | Statistical Analysis

Statistical analysis was carried out as indicated in each figure legend using GraphPad Prism 9 (GraphPad Software) and R version 4.2.2 [28]. Linear mixed models were performed using the lmerTest package and post hoc comparison with the emmeans package in R version 4.2.2. The number of biological replicates is stated in the figure legends. No power calculations were performed, and the sample sizes were not predetermined.

## 3 | Results

### 3.1 | Inhibition of FAK Y397 Phosphorylation Is Associated With Impaired Glucose Uptake Independent of Insulin Signaling

To assess the effect of acute FAKi treatment on FAK autophosphorylation, we measured FAK phosphorylation on site Y397 in primary adipocytes after short-term incubation with FAK inhibitor PF-573228. Western blot analysis showed reduced FAK Y397 phosphorylation after 1 h of FAKi treatment, in a dose-dependent manner (Figure 1A,B). A 70–80% decrease in FAK Y397 phosphorylation was detected at 10 μM FAKi compared to control (DMSO-treated) cells under basal as well as insulin-stimulated conditions (Figure 1A,B). Although this reduction appeared more pronounced under insulin-stimulated conditions, we found no significant interaction effect of FAKi and Insulin (Interaction: FAKi × Insulin: *p*-value ~0.0786). Additionally, we observed a slight, although not significant, increase in FAK phosphorylation upon insulin treatment. Using a glucose-tracer assay, we discovered that FAKi treatment decreased both basal and insulin-stimulated glucose uptake (Figure 1C). Indeed, glucose uptake was reduced by ~50% after pre-incubation with 10 μM FAKi (Figure 1C, each experiment displayed in Figure S1B). These findings were reproducible in

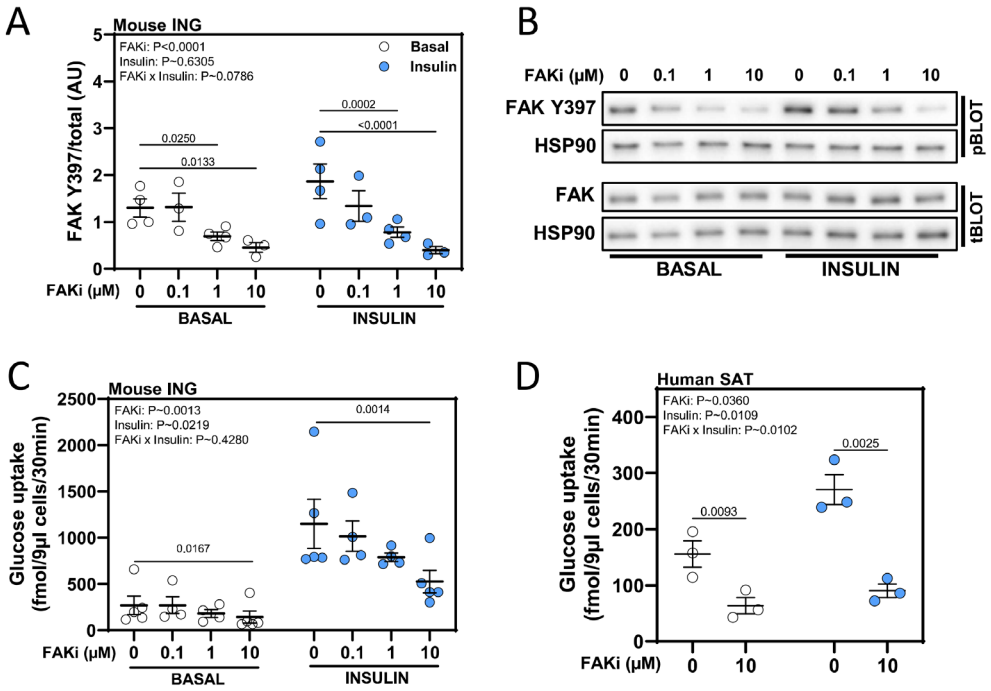


**FIGURE 1** | (A) Quantification of FAK Y397 phosphorylation (western blotting) in primary, inguinal mouse adipocytes after 1 h pre-incubation with respective doses of FAKi (or DMSO, control) and subsequent incubation with (30 min, 10 nM) or without insulin; data shown as mean ± SEM and $n = 3–4$. (B) Representative western blots of FAK Y397 and total FAK. Heat shock protein 90 (HSP90) was used as the loading control. (C) Glucose uptake in primary, inguinal mouse or (D) primary human, subcutaneous adipocytes after 1 h pre-incubation with respective doses of FAKi and subsequent incubation with (30 min, 10 nM) or without insulin; $n = 3–5$; data shown as mean ± SEM. Data in (A) and (C) were analyzed using mixed effects analysis, including a random subject effect (mouse) and fixed effects of stimulation (insulin) and condition (FAKi). Interaction effects of insulin and FAK inhibitor (FAKi × Insulin) were evaluated. (D) was analyzed using a repeated-measures two-way ANOVA. The effects of insulin, FAKi, and FAKi × Insulin were investigated. Bonferroni multiple comparison adjustment ($\alpha = 0.05$) was used in the post hoc analysis of (A, C, and D). Insulin-stimulated conditions are displayed in blue. The glucose uptake outcome in (C) was log-transformed for statistical analysis.

human primary subcutaneous adipocytes, where we observed a similar reduction in glucose uptake upon pre-incubation with 10 μM FAKi, and a significant interaction effect of FAKi and insulin treatment (FAKi × Insulin: *p*-value ~0.0102, Figure 1D). Additionally, we found that a short-term (5 min) pre-treatment with FAKi had similar effects on glucose uptake as the 1-h pre-treatment (Figure S1C). No cytotoxic effect of FAKi was observed at the used concentrations (measured by lactate-dehydrogenase release; Figure S1D).

Interestingly, pre-treatment with 10 μM FAKi compared to DMSO (control) treatment induced no changes in either non- or insulin-stimulated (10 nM, 5 min) phosphorylation of the canonical insulin signaling targets, IRS-1 Y612, PKB S473 and T308, or AS160 T642 (Figure 2A,B). In contrast, we found a clear reduction in mitogenic signaling, where ERK 1/2 phosphorylation at T202/Y204 decreased ~50% in both basal and insulin-stimulated conditions (Figure 2A,B). These findings from mouse adipocytes were reproducible in human adipocytes, where we observed no differences in PKB and AS160 phosphorylation but a clear reduction in ERK 1/2 phosphorylation following pre-treatment with FAKi (Figure 2C). In line with the findings in (Figure 1A,B), FAK Y397 phosphorylation was diminished in FAKi-treated cells compared to control, whereas insulin alone induced a slight, but not significant increase in FAK Y397 phosphorylation (Figure 2A,B).

### 3.2 | Inhibition of FAK Y397 Autophosphorylation Leads to Reduced Association of FAK With Cytoskeletal Proteins

Next, we applied affinity-purification combined with quantitative mass spectrometry to monitor FAK interactions. Primary adipocytes remained either untreated (DMSO, no insulin stimulation) throughout or were pre-incubated with either 10 μM FAKi (FAKi + insulin) or DMSO (DMSO + insulin) prior insulin treatment. Thereafter, we performed immunoprecipitation of FAK and subsequently analyzed samples using liquid chromatography–tandem mass spectrometry. Successful immunoprecipitation of FAK was confirmed by western blotting (Figure 3A). Insulin-stimulation alone induced only minor changes in FAK-binding partners, including Ca4, Gnai1, Gnai2, Gnb1, Rpl36, and Purb (Figure 3B). In contrast, pre-treatment with 10 μM FAKi (FAKi + insulin vs. DMSO + insulin) changed binding between FAK and 17 proteins (Figure 3C) associated with the significantly enriched "intracellular anatomical structure" GO term. STRING network analysis revealed strong functional and physical protein associations between 15 of these proteins, with 13 of them belonging to the enriched "cytoskeleton" GO term (Figure 3D). Interestingly, the protein interactions between FAK-Arp2/3 (Arpc2/Arpc4) were among the most significantly affected by FAKi-treatment (Figure 3C).

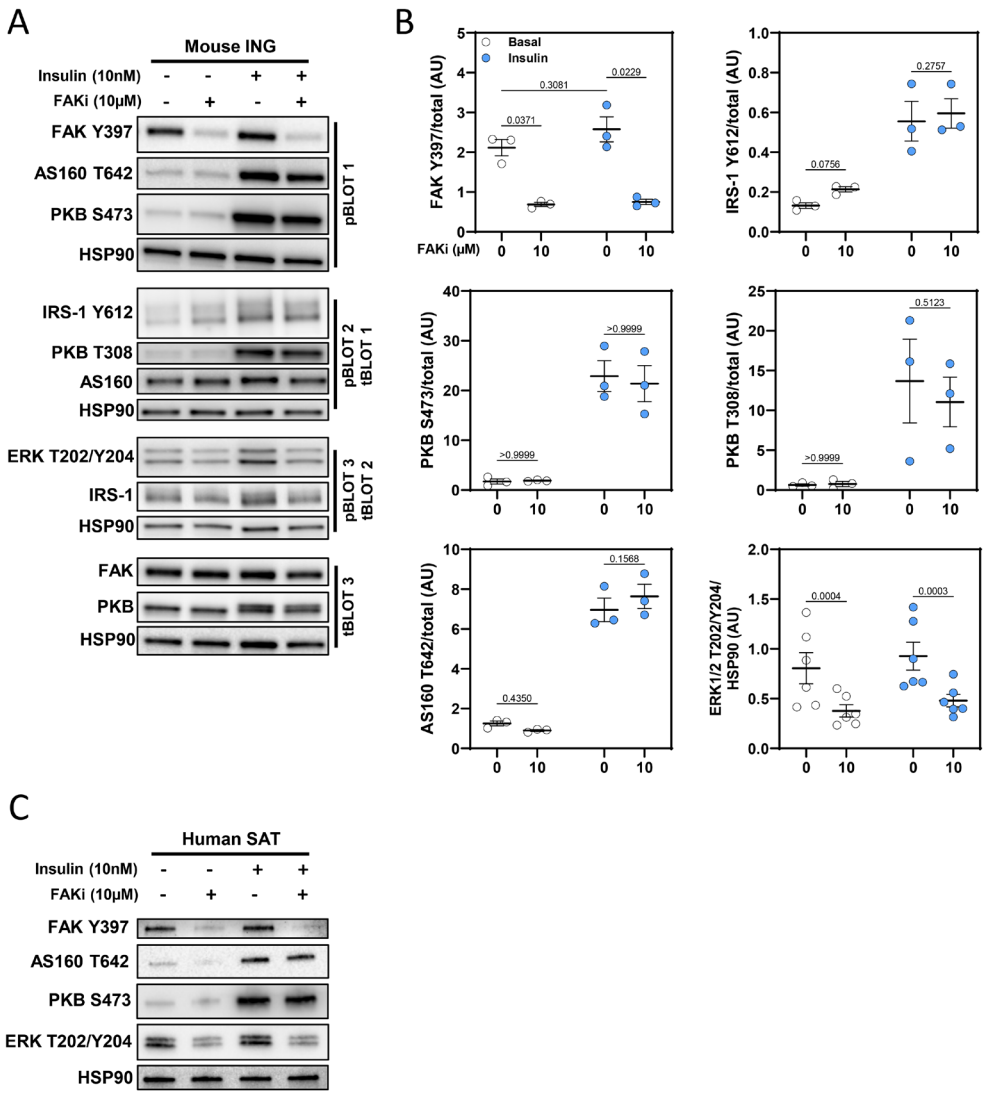


**FIGURE 2** | (A) Representative western blots of insulin signaling targets in primary, inguinal mouse adipocytes after 1 h pre-treatment with 10 μM FAKi and subsequent incubation with (5 min, 10 nM) or without insulin. (B) Corresponding quantifications of FAK Y397 ($n = 3$), IRS-1 Y612 ($n = 3$), PKB S473/T308 ($n = 3$), AS160 T642 ($n = 3$) and ERK1/2 T202/Y204 ($n = 6$) phosphorylation; data shown as mean ± SEM. Statistical analysis was performed using two-way repeated measures ANOVA with Bonferroni multiple comparison adjustment ($\alpha = 0.05$). (C) Representative western blots of FAK Y397, PKB S473, AS160 T642, and ERK1/2 T202/Y204 in primary human subcutaneous adipocytes after 1 h pre-treatment with 10 μM FAKi and subsequent incubation with (5 min, 10 nM) or without insulin; $n = 1$.

### 3.3 | Inhibition of FAK Y397 Autophosphorylation Leads to Impaired GLUT4 Translocation in a Rac1-Dependent Way

Since Arp2/3 complex activity is proposed to regulate GLUT4 translocation in an actin-dependent way [29], we next investigated whether FAKi treatment exerted effects on GLUT4 translocation. For that, we used an antibody that recognizes the extracellular epitope of endogenous GLUT4 (LM048, [27]), thus only detecting GLUT4 translocated and inserted into the plasma membrane. As expected, we found a significant increase in the LM048 signal with insulin compared to non-stimulated cells (two-fold increase, Figure 3E). Interestingly, we detected an apparent decrease (~50%) in LM048 signal in cells pre-incubated with 10 μM FAKi prior to insulin stimulation (Figure 3E). An experiment illustrating individual cell-to-cell variation and representative microscopy images are shown in Figure 3E (middle and right panels).

To investigate the importance of Arp2/3, we made use of the selective Arp2/3 complex inhibitor CK666. Pre-treatment with 100 μM CK666 caused a significant decrease in insulin-stimulated glucose uptake in both mouse (Figure 3F) and human (Figure 3G) adipocytes. To further assess FAK-mediated effects on cytoskeletal dynamics in adipocytes, we assayed the activity of Rac1, a small GTPase crucial for cytoskeleton remodeling and GLUT4 translocation [30]. Rac1-GTPase activity has previously been shown to be controlled by FAK in non-adipocyte cell types [31]. Here, we found that insulin treatment induced a two-fold increase in Rac1 GTP-loading in primary mouse adipocytes, while pre-treatment with 10 μM FAKi decreased insulin-stimulated Rac1 GTP-loading ~40% and basal Rac1 activity

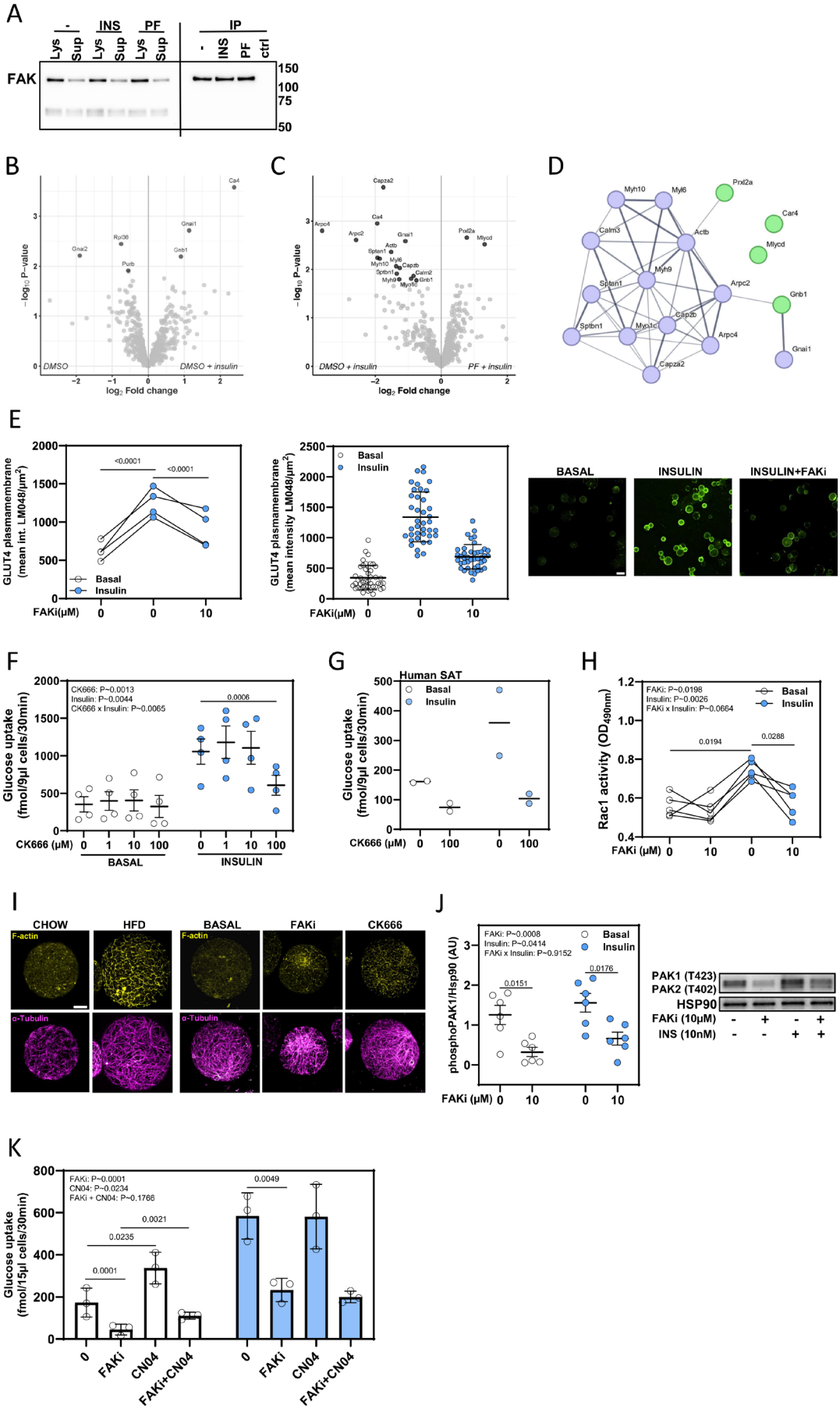


**FIGURE 3** | Legend on next page.

**FIGURE 3** | (A) Western blot of total FAK after FAK immunoprecipitation in primary, inguinal mouse adipocytes treated with DMSO (–), 10 nM insulin (INS), or 10 μM FAKi (PF); crtl = rabbit-IgG control. Input cell lysates (Lys) and supernatants after FAK IP (SUP) and immunoprecipitated samples (IP) were loaded to confirm successful pull-down. (B) Volcano plot displaying FAK-associated proteins; contrasting DMSO and DMSO + insulin conditions to investigate the effects of insulin stimulation. Proteins that show significant differences (FDR < 0.05 and a log2 fold change > 0.5) are highlighted and labeled with names ($n = 3$). (C) Volcano plot displaying FAK-associated proteins contrasting DMSO + insulin and PF + insulin conditions to investigate the effects of FAKi treatment. Proteins that show significant differences (FDR < 0.05 and a log2 fold change > 0.5) are highlighted and labeled with names ($n = 3$). (D) STRING network of proteins showing significant differences in the PF + insulin versus DMSO + insulin contrast. Nodes are labeled with corresponding protein names. The edges represent both functional and physical protein associations, with line thickness indicating the strength of data support (confidence score 0.4–1.0). Proteins associated with the enriched "cytoskeleton" GO cellular component term (GO:0005856) are marked in blue. (E, left panel) Quantification of LM048 GLUT4 intensity per area in primary, epididymal mouse adipocytes treated with DMSO (Basal, 0), 10 nM insulin (Insulin, 0), or 10 μM FAKi + 10 nM insulin (Insulin, 10) in $n = 4$ experiments; the mean intensity of 30 cells per experiment was averaged and analyzed. Statistical analysis was carried out using linear mixed models in R. Bonferroni multiple comparison adjustment was used for post hoc analysis, $\alpha = 0.05$. For statistical analysis, the mean intensity was log-transformed. (E, middle panel) Corresponding quantification of LM048 GLUT4 intensity per area in approximately 30 cells for one experiment to visualize cell-to-cell variation, displayed as mean ± SD. (E, right panel) Representative confocal images of LM048-stained epididymal adipocytes. Scale bar = 100 μm. (F) Glucose uptake in primary inguinal mouse and (G) subcutaneous human adipocytes after 1 h pre-incubation with respective doses of CK666 and subsequent incubation with (30 min, 10 nM) or without insulin; $n = 4$ in (F) and $n = 2$ in (G); Statistical analysis in (F) was carried out using repeated measures two-way ANOVA. The effect of stimulation (Insulin), condition (CK666), and interaction of insulin and CK666 (CK666 × Insulin) were evaluated. Bonferroni multiple comparison adjustment was used for post hoc analysis, $\alpha = 0.05$. (H) Rac1 activity assay in primary, inguinal mouse adipocytes after treatment with 10 μM FAKi (1 h) and subsequent incubation with (5 min, 10 nM) or without insulin. Statistical analysis in H) was carried out using repeated measures two-way ANOVA. The effects of stimulation (Insulin), condition (FAKi), and interaction of insulin and FAKi (FAKi × Insulin) were evaluated. Bonferroni multiple comparison adjustment was used for post hoc analysis, $\alpha = 0.05$, $n = 3$. (I, left panel) Confocal images of F-actin tracers (yellow, phalloidin) and microtubules (purple, alpha-tubulin) in inguinal adipocytes from either chow-fed or mice fed a high-fat diet (HFD, 10 weeks); scale bar = 20 μm. (I, right panel) Confocal images of primary, inguinal adipocytes incubated with (10 μM, 1 h) or without FAKi from mice fed a high-fat diet (10 weeks). (J) Western blot of p21-activated kinase (PAK) phosphorylation and corresponding quantification in primary, inguinal mouse adipocytes after pre-treatment with 10 μM FAKi for 1 h; samples were subsequently insulin-stimulated (10 nM, 5 min) or remained non-stimulated. Statistical analysis was carried out using repeated measures two-way ANOVA. The effects of stimulation (Insulin), condition (FAKi), and interaction of insulin and FAKi (FAKi × Insulin) were evaluated. Bonferroni multiple comparison adjustment was used for post hoc analysis, $\alpha = 0.05$, $n = 6$; mean ± SEM. (K) Glucose uptake in primary, inguinal mouse adipocytes after 1 h pre-incubation with DMSO control (0), 10 μM FAKi (FAKi), 1 μg/mL CN04 (CN04), or 10 μM FAKi and 1 μg/mL CN04 (FAKi + CN04) combined and subsequent incubation with (10 nM, 30 min) or without insulin; $n = 3$. Statistical analysis was carried out using linear mixed models in R. The glucose uptake outcome was log-transformed for statistical analysis. A random subject effect (mouse), as well as fixed effects of stimulation (insulin) and condition (FAKi, CN04, and FAKi + CN04), were included. No multiple comparison adjustment was used in post hoc analysis.

~10% (Figure 3H). Although this reduction appeared more pronounced under insulin-stimulated conditions, it did not reach significance (Interaction: FAKi × Insulin $p$-value: ~0.0644).

Using confocal microscopy, we further investigated changes in cytoskeletal organization and found that FAK inhibition evoked no endpoint changes in the abundance of filamentous actin or microtubules (Figure 3I), suggesting a mechanism that is restricted to actin turnover rather than changes in the net ratio between globular/filamentous actin. Using western blotting, we assessed the phosphorylation of Rac1 downstream targets and found a significant inhibition of p21-activated kinase (PAK) phosphorylation (Figure 3J) upon pre-treatment with FAKi, while we observed no FAKi-induced changes in phosphorylation of Arp2 T237/T238 or Cofilin1 S3 protein levels (Figure S1E). Next, we made use of the Rho/Rac/Cdc42 activator CN04 to investigate whether restoration of the Rac1 GTP-loading levels could restore the FAKi-induced impairment in glucose uptake. Interestingly, we found that CN04 treatment itself induced a significant increase in basal glucose uptake (Figure 3K). Further, we observed that the FAKi-induced reduction in basal glucose uptake was restored by ~70% with CN04 treatment (Figure 3K). No such effects were found under insulin-stimulated conditions (Figure 3K). These findings highlight the importance of Rac1 activity for glucose uptake in adipocytes and provide evidence that FAK exerts its effect on glucose transport via Rac1.

## 4 | Discussion

Understanding the mechanisms coordinating extra- to intracellular signaling is essential to resolve the contribution of impaired adipocyte function to systemic insulin resistance and obesity. One of the proteins connecting changes in the extracellular environment to intracellular adaptations is FAK [11].

Herein, we demonstrate that inhibition of FAK autophosphorylation is associated with decreased glucose uptake and impaired GLUT4 translocation in adipocytes. Bisht et al. and Huang et al. have previously demonstrated the importance of FAK for insulin-stimulated GLUT4 translocation in skeletal muscle [12, 16]. Notably, the authors examined the effects of total FAK expression rather than the state of FAK phosphorylation in those studies [18]. Using affinity purification of FAK-binding proteins combined with quantitative mass spectrometry, we found that FAK inhibition almost exclusively affected the association of FAK with proteins involved in cytoskeletal organization. These findings fit a number of studies demonstrating

a central role of FAK in cytoskeletal remodeling [11, 12, 32]. Other studies have also demonstrated that insulin regulates actin remodeling, which in turn is essential to sustain GLUT4 translocation and GSV fusion with the plasma membrane [10, 30, 33–35]. Our findings demonstrate that FAK inhibition diminished the association between FAK and the actin nucleator Arp2/3 complex and led to reduced Rac1 activation, both of which are key nodes for actin turnover [29, 30, 36]. Further, we provide evidence for the importance of actin turnover for adipocyte glucose uptake using an Arp2/3 complex inhibitor. Together, this implies that FAK regulates GLUT4 translocation and glucose transport in primary adipocytes by regulating cytoskeletal turnover. This is in line with a study by Cai et al. showing that conditional beta-cell specific FAK knockdown impaired insulin secretion via reduced cortical actin polymerization, leading to impaired exocytosis and fusion of insulin granules [37]. Also, in the study by Bisht et al. modulation of FAK expression altered insulin-mediated actin remodeling, thereby affecting GLUT4 exocytosis [12]. In their study, insulin was shown to induce a redistribution of FAK to sites where actin remodeling occurred, forming insulin signaling hubs that also harbored GLUT4, facilitating GLUT4 exocytosis. Although not tested herein, a similar FAK redistribution might occur in adipocytes. While Bisht et al. and others have proposed that FAK influences the canonical insulin signaling cascade in skeletal muscle [15, 37], we found no evident changes in phosphorylation of IRS-1 Y612, PKB S473 and T308 or AS160 T642 following inhibitor treatment in adipocytes. Therefore, we conclude that the reduced insulin-stimulated glucose uptake cannot be a mere consequence of impaired insulin signaling. Rather, FAK inhibition affects glucose transport via cytoskeleton remodeling [38]. Accordingly, we previously demonstrated improved insulin-stimulated glucose transport via changes in cytoskeleton remodeling, independent of insulin signaling in primary adipocytes [38]. This is further supported by our findings showing that insulin-stimulated Rac1 GTP-loading is diminished under FAKi-treated conditions, and further that the insulin-induced phosphorylation of the Rac1 downstream target PAK is decreased upon FAKi treatment. Furthermore, we show that Rac1/Rho/Cdc42 activation increases basal glucose uptake and partially restores FAKi-induced reduction in basal glucose uptake. Rac1 is a small GTPase that regulates insulin-stimulated glucose uptake in skeletal muscle and adipocytes, likely via its effects on the actin cytoskeleton and GLUT4 translocation [30, 39]. In line with our findings here, Chiu et al. demonstrated that FAK Y397 phosphorylation is critical for FAK-promoted Rac1 activation [40], and Chang et al. showed that FAK facilitates the activation and translocation of Rac1 to focal adhesions through the tyrosine phosphorylation of βPIX [41]. This suggests that Rac1 is indeed a central node in the FAKi-mediated effects on adipocyte glucose uptake. Possibly, the lack of a restorative effect using a Rac1 activator in the insulin-stimulated state could arise from different actin-dependent GLUT4 recycling mechanisms, where insulin promotes rapid GLUT4 vesicle fusion in a transient fashion, distinct from GLUT4 exocytosis in the basal state, forming GLUT4 clusters [42]. Intriguingly, we did observe a trend towards an insulin-mediated increase in FAK Y397 phosphorylation. Also, insulin potentiated the FAKi-induced Rac1 inhibition. Together, these findings point towards a mechanism where insulin accelerates actin remodeling, which in turn potentiates the inhibitory effect of FAKi on cytoskeletal turnover. While these observations did not reach statistical significance, they urge for further studies addressing a potential role of insulin-regulated FAK activity.

In a study by Luk et al. adipocyte-specific FAK knockdown led to systemic insulin resistance in mice, potentially due to reduced adipocyte survival [17]. Although we detected an apparent reduction in ERK1/2 phosphorylation with FAK inhibition, we found no induction of cytotoxicity upon short-term incubation with a FAKi. In line with our findings, ERK has been shown to regulate phosphorylation of the WAVE2 Regulatory Complex and thereby its binding to Arp2/3, promoting actin polymerization [43]. This impairment in ERK phosphorylation could also play a role in actin dynamics in adipocytes. Ridyard et al. highlight that FAK manipulation induces cytoskeletal changes without altering apoptosis in chick embryo cells [44]. Nevertheless, we cannot rule out the possible involvement of FAKi-induced cellular apoptosis and its contribution to impaired glucose metabolism [17, 21].

In summary, our findings indicate that inhibition of FAK autophosphorylation leads to diminished glucose uptake via impairment of cytoskeletal turnover, likely attributed to changes in Rac1 activity and Arp2/3 function, and consequent disruption of GLUT4 translocation in adipocytes.

### Author Contributions

F.K., M.N., and K.G.S. conceived and designed the experiments. F.K., M.N., and A.B.-M. performed the experiments and acquired the data. D.K., F.K., M.N., A.B.-M., and K.G.S. analyzed, interpreted, and critically revised the data. M.N. drafted the manuscript. All authors revised the manuscript and approved the final version. We certify that the submission is original work and is not under review at any other publication.

### Acknowledgments

This work was financially supported by the Swedish Research Council (2023-01779) and Strategic Research Area EXODIAB (2009-1039), the Swedish Foundation for Strategic Research (IRC15-0067), Novo Nordisk (NNF20OC0063659), Swedish Diabetes Foundation, The Royal Physiographic Society of Lund, and Albert Påhlsson Foundation. Support from the Swedish National Infrastructure for Biological Mass Spectrometry (BioMS) is gratefully acknowledged. We also thank the LUDC Bioinformatics Unit for computational and analytical support, and Lund University Bioimaging Center (LBIC) for technical support.

### Ethics Statement

Studies on human adipose tissue were approved by the Regional Ethical Review Boards at Lund University (approval number 2017/920). All animal procedures were reviewed and approved by the Malmö / Lund Committee for Animal Experiment Ethics, approval number 5.8.18-00497/2020.

### Consent

Abdominal subcutaneous adipose tissue was collected from women who underwent reconstructive breast surgery at Scania University Hospital in Sweden. The participants were given written and oral information about the study before providing their informed, written consent. Human studies were approved by the Regional Ethical Review Boards at Lund University (approval number 2017/920).

## Conflicts of Interest

The authors declare no conflicts of interest.

## Data Availability Statement

The data that support the findings of this study are available on request from the corresponding author. The analysis code for IP-MS is available at: https://github.com/LUDC-bioinformatics/proteomic_FAK_adipose.

## References


1. C. E. Hagberg and K. L. Spalding, "White Adipocyte Dysfunction and Obesity-Associated Pathologies in Humans," *Nature Reviews. Molecular Cell Biology* 25 (2023), https://doi.org/10.1038/s41580-023-00680-1.

2. D. E. James, J. Stöckli, and M. J. Birnbaum, "The Aetiology and Molecular Landscape of Insulin Resistance," *Nature Reviews. Molecular Cell Biology* 22 (2021), https://doi.org/10.1038/s41580-021-00390-6.

3. M. Kanzaki and J. E. Pessin, "Insulin-Stimulated GLUT4 Translocation in Adipocytes Is Dependent Upon Cortical Actin Remodeling," *Journal of Biological Chemistry* 276, no. 45 (2001): 42436–42444, https://doi.org/10.1074/jbc.M108297200.

4. J. A. Lopez, J. G. Burchfield, D. H. Blair, et al., "Identification of a Distal GLUT4 Trafficking Event Controlled by Actin Polymerization," *Molecular Biology of the Cell* 20, no. 17 (2009): 3918–3929, https://doi.org/10.1091/mbc.E09-03-0187.

5. J. Brozinick, B. Berkemeier, and J. Elmendorf, "'Acting' on GLUT4:Membrane & Cytoskeletal Components of Insulin Action," *Current Diabetes Reviews* 3, no. 2 (2007), https://doi.org/10.2174/157339907780598199.

6. K. A. DeMali, K. Wennerberg, and K. Burridge, "Integrin Signaling to the Actin Cytoskeleton," *Current Opinion in Cell Biology* 15 (2003), https://doi.org/10.1016/S0955-0674(03)00109-1.

7. I. Delon and N. H. Brown, "Integrins and the Actin Cytoskeleton," *Current Opinion in Cell Biology* 19 (2007), https://doi.org/10.1016/j.ceb.2006.12.013.

8. K. Sun, X. Li, and P. E. Scherer, "Extracellular Matrix (ECM) and Fibrosis in Adipose Tissue: Overview and Perspectives," *Comprehensive Physiology* 13, no. 1 (2023), https://doi.org/10.1002/cphy.c220020.

9. G. Marcelin, E. L. Gautier, and K. Clement, "Adipose Tissue Fibrosis in Obesity: Etiology and Challenges," *Annual Review of Physiology* 84 (2022), https://doi.org/10.1146/annurev-physiol-060721-092930.

10. B. Hansson, B. Morén, C. Fryklund, et al., "Adipose Cell Size Changes Are Associated With a Drastic Actin Remodeling," *Scientific Reports* 9, no. 1 (2019): 12941, https://doi.org/10.1038/s41598-019-49418-0.

11. S. K. Mitra, D. A. Hanson, and D. D. Schlaepfer, "Focal Adhesion Kinase: In Command and Control of Cell Motility," *Nature Reviews. Molecular Cell Biology* 6 (2005), https://doi.org/10.1038/nrm1549.

12. B. Bisht and C. S. Dey, "Focal Adhesion Kinase Contributes to Insulin-Induced Actin Reorganization Into a Mesh Harboring Glucose Transporter-4 in Insulin Resistant Skeletal Muscle Cells," *BMC Cell Biology* 9 (2008): 48, https://doi.org/10.1186/1471-2121-9-48.

13. F. Draicchio, V. Behrends, N. A. Tillin, N. M. Hurren, L. Sylow, and R. Mackenzie, "Involvement of the Extracellular Matrix and Integrin Signalling Proteins in Skeletal Muscle Glucose Uptake," *Journal of Physiology* 600, no. 20 (2022), https://doi.org/10.1113/JP283039.

14. B. Bisht, K. Srinivasan, and C. S. Dey, "In Vivo Inhibition of Focal Adhesion Kinase Causes Insulin Resistance," *Journal of Physiology* 586, no. 16 (2008): 3825–3837, https://doi.org/10.1113/jphysiol.2008.157107.

15. B. Bisht, H. L. Goel, and C. S. Dey, "Focal Adhesion Kinase Regulates Insulin Resistance in Skeletal Muscle," *Diabetologia* 50, no. 5 (2007): 1058–1069, https://doi.org/10.1007/s00125-007-0591-6.

16. D. Huang, M. Khoe, D. Ilic, and M. Bryer-Ash, "Reduced Expression of Focal Adhesion Kinase Disrupts Insulin Action in Skeletal Muscle Cells," *Endocrinology* 147, no. 7 (2006): 3333–3343, https://doi.org/10.1210/en.2005-0382.

17. C. T. Luk, S. Y. Shi, E. P. Cai, et al., "FAK Signalling Controls Insulin Sensitivity Through Regulation of Adipocyte Survival," *Nature Communications* 8 (2017): 14360, https://doi.org/10.1038/ncomms14360.

18. D. Chen, J. S. Elmendorf, A. L. Olson, X. Li, H. S. Earp, and J. E. Pessin, "Osmotic Shock Stimulates GLUT4 Translocation in 3T3L1 Adipocytes by a Novel Tyrosine Kinase Pathway," *Journal of Biological Chemistry* 272, no. 43 (1997): 27401–27410, https://doi.org/10.1074/jbc.272.43.27401.

19. F. Ding, P. Zheng, H.-T. Fang, et al., "Adipocyte-Specific FAK Deletion Promotes Pancreatic β-Cell Apoptosis via Adipose Inflammatory Response to Exacerbate Diabetes Mellitus," *Clinical and Translational Medicine* 14 (2024): e1742.

20. J. Shin, S. Toyoda, Y. Okuno, et al., "HSP47 Levels Determine the Degree of Body Adiposity," *Nature Communications* 14, no. 1 (2023): 7319, https://doi.org/10.1038/s41467-023-43080-x.

21. H. j. Chen, X. y. Yan, A. Sun, L. Zhang, J. Zhang, and Y. e. Yan, "High-Fat-Diet-Induced Extracellular Matrix Deposition Regulates Integrin—FAK Signals in Adipose Tissue to Promote Obesity," *Molecular Nutrition & Food Research* 66, no. 7 (2022), https://doi.org/10.1002/mnfr.202101088.

22. M. Rodbell, "The Metabolism of Isolated Fat Cells," *Journal of Biological Chemistry* 241, no. 17 (1966): 3909–3917, https://doi.org/10.1016/s0021-9258(18)99793-0.

23. J. Gliemann, W. D. Rees, and J. A. Foley, "The Fate of Labelled Glucose Molecules in the Rat Adipocyte. Dependence on Glucose Concentration," *Biochimica et Biophysica Acta, Molecular Cell Research* 804, no. 1 (1984), https://doi.org/10.1016/0167-4889(84)90100-9.

24. K. F. Cho, T. C. Branon, N. D. Udeshi, S. A. Myers, S. A. Carr, and A. Y. Ting, "Proximity Labeling in Mammalian Cells With TurboID and Split-TurboID," *Nature Protocols* 15, no. 12 (2020): 3971–3999, https://doi.org/10.1038/s41596-020-0399-0.

25. X. Zhang, A. H. Smits, G. B. A. Van Tilburg, H. Ovaa, W. Huber, and M. Vermeulen, "Proteome-Wide Identification of Ubiquitin Interactions Using UbIA-MS," *Nature Protocols* 13, no. 3 (2018): 530–550, https://doi.org/10.1038/nprot.2017.147.

26. D. Szklarczyk, A. L. Gable, D. Lyon, et al., "STRING v11: Protein-Protein Association Networks With Increased Coverage, Supporting Functional Discovery in Genome-Wide Experimental Datasets," *Nucleic Acids Research* 47, no. D1 (2019): D607–D613, https://doi.org/10.1093/nar/gky1131.

27. D. F. Tucker, J. T. Sullivan, K. A. Mattia, et al., "Isolation of State-Dependent Monoclonal Antibodies Against the 12-Transmembrane Domain Glucose Transporter 4 Using Virus-Like Particles," *Proceedings of the National Academy of Sciences of the United States of America* 115, no. 22 (2018): E4990–E4999, https://doi.org/10.1073/pnas.1716788115.

28. R Core Team, "R: A Language and Environment for Statistical Computing," 2019.

29. T. T. Chiu, N. Patel, A. E. Shaw, J. R. Bamburg, and A. Klip, "Arp2/3- and Cofilin-Coordinated Actin Dynamics Is Required for Insulin-Mediated GLUT4 Translocation to the Surface of Muscle Cells," *Molecular Biology of the Cell* 21, no. 20 (2010): 3529–3539, https://doi.org/10.1091/mbc.E10-04-0316.

30. N. Takenaka, M. Nakao, S. Matsui, and T. Satoh, "A Crucial Role for the Small GTPase rac1 Downstream of the Protein Kinase Akt2 in Insulin Signaling That Regulates Glucose Uptake in Mouse Adipocytes," *International Journal of Molecular Sciences* 20, no. 21 (2019): 5443, https://doi.org/10.3390/ijms20215443.

31. J. T. Parsons, A. R. Horwitz, and M. A. Schwartz, "Cell Adhesion: Integrating Cytoskeletal Dynamics and Cellular Tension," *Nature Reviews. Molecular Cell Biology* 11 (2010), https://doi.org/10.1038/nrm2957.

32. B. Fabry, A. H. Klemm, S. Kienle, T. E. Schäffer, and W. H. Goldmann, "Focal Adhesion Kinase Stabilizes the Cytoskeleton," *Biophysical Journal* 101, no. 9 (2011): 2131–2138, https://doi.org/10.1016/j.bpj.2011.09.043.

33. W. Yang, S. Thein, C. Y. Lim, et al., "Arp2/3 Complex Regulates Adipogenesis by Controlling Cortical Actin Remodelling," *Biochemical Journal* 464, no. 2 (2014): 179–192, https://doi.org/10.1042/BJ20140805.

34. J. Huang, T. Imamura, J. L. Babendure, J. C. Lu, and J. M. Olefsky, "Disruption of Microtubules Ablates the Specificity of Insulin Signaling to GLUT4 Translocation in 3T3-L1 Adipocytes," *Journal of Biological Chemistry* 280, no. 51 (2005): 42300–42306, https://doi.org/10.1074/jbc.M510920200.

35. P. Vollenweider, S. S. Martin, T. Haruta, et al., "The Small Guanosine Triphosphate-Binding Protein Rab4 Is Involved in Insulin-Induced GLUT4 Translocation and Actin Filament Rearrangement in 3T3- L1 Cells," *Endocrinology* 138, no. 11 (1997): 4941–4949, https://doi.org/10.1210/endo.138.11.5493.

36. E. D. Goley and M. D. Welch, "The ARP2/3 Complex: An Actin Nucleator Comes of Age," *Nature Reviews. Molecular Cell Biology* 7 (2006), https://doi.org/10.1038/nrm2026.

37. E. P. Cai, M. Casimir, S. A. Schroer, et al., "In Vivo Role of Focal Adhesion Kinase in Regulating Pancreatic β-Cell Mass and Function Through Insulin Signaling, Actin Dynamics, and Granule Trafficking," *Diabetes* 61, no. 7 (2012): 1708–1718, https://doi.org/10.2337/db11-1344.

38. C. Fryklund, B. Morén, M. Neuhaus, V. Periwal, and K. G. Stenkula, "Rosiglitazone Treatment Enhances Intracellular Actin Dynamics and Glucose Transport in Hypertrophic Adipocytes," *Life Sciences* 299 (2022): 120537, https://doi.org/10.1016/j.lfs.2022.120537.

39. L. Sylow, T. E. Jensen, M. Kleinert, et al., "Rac1 Signaling Is Required for Insulin-Stimulated Glucose Uptake and Is Dysregulated in Insulin-Resistant Murine and Human Skeletal Muscle," *Diabetes* 62, no. 6 (2013): 1865–1875, https://doi.org/10.2337/db12-1148.

40. Y. W. Chiu, L. Y. Liou, P. T. Chen, et al., "Tyrosine 397 Phosphorylation Is Critical for FAK-Promoted Rac1 Activation and Invasive Properties in Oral Squamous Cell Carcinoma Cells," *Laboratory Investigation* 96, no. 3 (2016): 296–306, https://doi.org/10.1038/labinvest.2015.151.

41. F. Chang, C. A. Lemmon, D. Park, and L. H. Romer, "FAK Potentiates Rac1 Activation and Localization to Matrix Adhesion Sites: A Role for βPIX," *Molecular Biology of the Cell* 18, no. 1 (2007): 253–264, https://doi.org/10.1091/mbc.E06-03-0207.

42. K. G. Stenkula, V. A. Lizunov, S. W. Cushman, and J. Zimmerberg, "Insulin Controls the Spatial Distribution of GLUT4 on the Cell Surface Through Regulation of Its Postfusion Dispersal," *Cell Metabolism* 12, no. 3 (2010): 250–259, https://doi.org/10.1016/j.cmet.2010.08.005.

43. M. C. Mendoza, E. E. Er, W. Zhang, et al., "ERK-MAPK Drives Lamellipodia Protrusion by Activating the WAVE2 Regulatory Complex," *Molecular Cell* 41, no. 6 (2011): 661–671, https://doi.org/10.1016/j.molcel.2011.02.031.

44. M. S. Ridyard and E. J. Sanders, "Inhibition of Focal Adhesion Kinase Expression Correlates With Changes in the Cytoskeleton but Not Apoptosis in Primary Cultures of Chick Embryo Cells," *Cell Biology International* 25, no. 3 (2001): 215–226, https://doi.org/10.1006/cbir.2000.0634.

**Supporting Information**

Additional supporting information can be found online in the Supporting Information section.